Simulating a Jammed Rotor Fault on SynRM and Integrate Results with Machine Learning

GEORGI ENCHEV, HRISTO MILUSHEV, NIKOLAY DJAGAROV
Electrical Department,
Nikola Vaptsarov Naval Academy,
Address: 73 Vasil Drumev str., Varna,
BULGARIA

Abstract: - The increasing use of synchronous reluctance motors (SynRM) in various types of electric drives is explained by its advantages. Different models of SynRM are used to study and control electric drives. In the article, a non-iterative model for electric drive research is proposed. Different types of faults can be simulated using this model. Jammed rotor fault mode is simulated. The obtained simulation results are diagnosed by machine learning, and the diagnosis accuracy is more than 98%.

Key-Words: **-** Synchronous, Reluctance, Motors, Mathematical, Model, Diagnosis, Machine, Learning, ML, AI.

Received: June 2, 2024. Revised: November 12, 2024. Accepted: March 9, 2025. Published: May 6, 2025.

1 Introduction

Synchronous reluctance (SynRM) motors combine the performance of a permanent magnet motor with the simplicity and service-friendliness of an asynchronous motor. The rotor consists only of a specially shaped magnetically conductive element. There are no windings and permanent magnets, therefore there is no power loss and there is easy maintenance. They have high power density and low cost. Furthermore, their use in adjustable electric drives ensures high efficiency, especially at partial load and high speed, [1], [2].

The SynRM motor is used in pumps, fans, compressors, propulsion, extruders, winders, conveyors, etc.

SynRM creates torque as a result of a change in magnetic resistance, with the magnetic flux taking the path of the lowest magnetic resistance. When the rotor and flux are out of phase, the magnetic torque rotates the rotor. The difference in magnetic resistance (saliency ratio) created by apparent polarity creates a magnetomotive force (MMF) that turns the rotor.

The disadvantage is torque ripple at low speed and quite a low power factor. As the saliency ratio increases, the power factor increases. Design modifications to the rotor have been proposed that change the L_d/L_q ratio, which increases the power factor.

Although the SynRM is a synchronous machine, unlike a conventional synchronous machine it can self-start on direct start.

Diagnostic methods for electrical machines are used for prevention, prediction, and repair. Vibration, temperature, and signature signals are used for diagnostics. Diagnostics are performed in the time and frequency domains. Finite element methods are also used. Numerous studies are known in the field of diagnostics of technical objects [3], [4], [5], [6], [7], [8], [9], [10], [11], [12], [13], [14], [15], [16], [17], [18], [19], [20], [21], [22], [23], [24], [25], [26], [27], [28].

Different models of SynRM are used to study and control electric drives. In the article, a non-iterative model for electric drive research is proposed. Different types of faults can be simulated using this model. Jammed rotor fault mode is simulated. The obtained simulation results are diagnosed by machine learning (ML).

2 Diagram of the Studied Electric Drive

The studied electric drive is a bow thruster used in ships. The heart of the drive is the synchronous reluctance motor which is fed by a diesel generator through frequency drive. The block scheme of the marine system is shown in Figure 1.

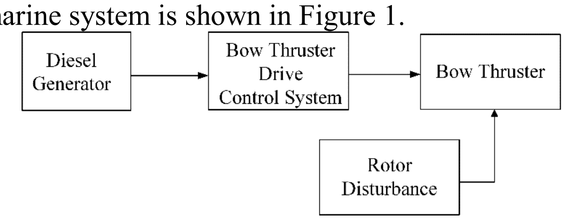

Fig. 1: Block scheme of the investigated system

Figure 2 shows the control strategy used in the bow thruster drive control system. The main blocks are: Outer Loop Control, where the speed deviation is estimated and formed by the reference currents in d-q axes; Current control, where the reference voltages in d-q axes are formed, which through the PWM Generator form the control pulses to the Inverter. A rotor disturbance is simulated to the shaft of the SynRM.

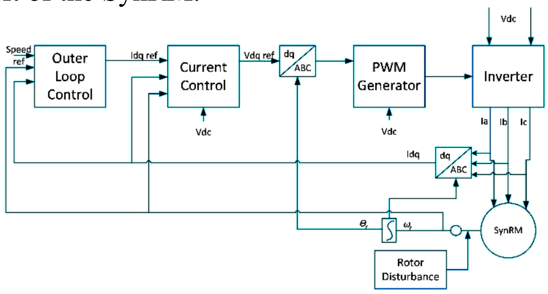

Fig. 2: SynRM control

3 SynRM Model

The use of SynRM mathematical models is mandatory when designing electric drives with this type of motor. Mathematical models allow their controllers to be designed and incorporated into drive control loops.

Different mathematical models differ in purpose, accuracy, state variables used, and form of representation, [29], [30], [31]. Almost all are represented in the d,q coordinate frame. A major difficulty in modeling is the nonlinear characteristics of the motor, and the dependence of L_d and L_q on the rotor position.

The article uses a model obtained by a method presented in [32].

Figure 3 shows the vector diagram of SynRM [1] in steady-state, which shows the main variables – voltage U, current I, and flux linkage ψ and their spatial position.

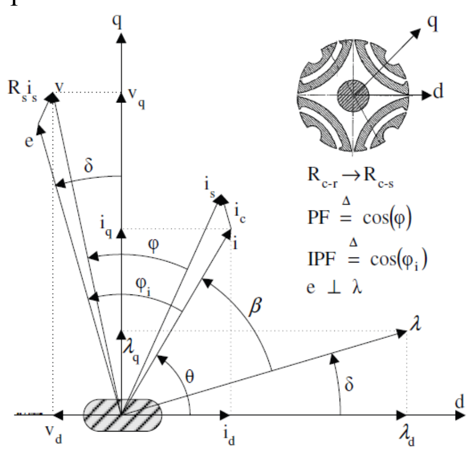

Fig. 3: Vector diagram of SynRM at steady-state, including the total iron losses truster torque

The mathematical model of the stator windings is written in the system of per units MF, in *d,q* frame, taking the standard assumptions [6]:

$$u_{sd} = R_s . i_{sd} + \frac{d}{dt}\psi_{sd} - \omega_r . \psi_q \quad (1)$$

$$u_{sq} = R_s . i_{sq} + \frac{d}{dt}\psi_{sq} + \omega_r . \psi_d \quad (2)$$

$$\psi_{sd}=L_d . i_{sd};\ \psi_{sq}=L_q . i_{sq}; \quad (3)$$

where:

R_s – stator resistance; L_d, L_q – stator inductance; ω_r – rotor angular speed; $L_d = L_s + M_s + 3/2L_m$; $L_q = L_s + M_s - 3/2L_m$; M_s – stator mutual inductance.

Equations (1) and (2) in matrix form:

$$\begin{bmatrix} u_d \\ u_q \end{bmatrix} = R_s . \begin{bmatrix} i_d \\ i_q \end{bmatrix} + \begin{bmatrix} L_d & 0 \\ 0 & L_q \end{bmatrix} . \frac{d}{dt}\begin{bmatrix} i_d \\ i_q \end{bmatrix} + \omega_r . \begin{bmatrix} 0 & -L_q \\ L_d & 0 \end{bmatrix} . \begin{bmatrix} i_d \\ i_q \end{bmatrix} \quad (4)$$

The motor rotation equation:

$$\frac{d}{dt}\omega_r = \frac{1}{\tau_m}(T_e - T_l - B_m . \omega_r) \quad (5)$$

where: τ_m – motor and load mechanical time constant; T_e – electromagnetic torque; T_l – load torque; B_m – rotor damping.

The electromagnetic torque of the motor:

$$T_e = (i_q . i_d , L_d - i_d . i_q . L_q) \quad (6)$$

$$\theta_r = \int \omega_r \, dt \quad (7)$$

After conversion into the form of the Cauchy system of equations (1) and (2) relative to the currents:

$$\frac{d}{dt}\begin{bmatrix} i_d \\ i_q \end{bmatrix} = \begin{bmatrix} a_{11} & a_{12} \\ a_{21} & a_{22} \end{bmatrix} . \begin{bmatrix} i_d \\ i_q \end{bmatrix} + \begin{bmatrix} b_{11} & 0 \\ 0 & b_{22} \end{bmatrix} . \begin{bmatrix} u_d \\ u_q \end{bmatrix} = \frac{d}{dt}\boldsymbol{I}_{mot} = \boldsymbol{A}_{mot} . \boldsymbol{I}_{mot} + \boldsymbol{B}_{mot} . \boldsymbol{U} \quad (8)$$

where: $a_{11}=-R_s/L_d$; $a_{12}=\omega_r . L_d/Lq$; $a_{21}=-\omega_r . L_d/L_q$; $a_{22}=-R_s/L_q$; $b_{11}=1/L_d$; $b_{22}=1/L_q$.

The SynRM equations are written in *d,q* frame to avoid variable motor parameters. However, the real values of the currents and voltages in the *a,b,c* frame are needed to determine the switching moments of the switches. Following is the inverter model and the corresponding *a,b,c→d,q→a,b,c* frame transformations. The inverter is modeled using switching functions, [33]:

$$\frac{d}{dt}\begin{bmatrix} i_a \\ i_b \\ i_c \end{bmatrix} = \frac{1}{L}.\begin{bmatrix} u_a \\ u_b \\ u_c \end{bmatrix} - \frac{R}{L}.\begin{bmatrix} i_a \\ i_b \\ i_c \end{bmatrix} - \frac{U_{dc}}{L}.\begin{bmatrix} \frac{(2S_a - S_b - S_c)}{3} \\ \frac{(2S_b - S_c - S_a)}{3} \\ \frac{(2S_c - S_a - S_b)}{3} \end{bmatrix}$$

$$\frac{d}{dt}\boldsymbol{I_{abc}} = \frac{1}{L}.\boldsymbol{U_{abc}} - \frac{R}{L}.\boldsymbol{I_{abc}} - \frac{U_{dc}}{L}.\boldsymbol{S} \qquad (9)$$

where: S_a, S_b, S_c – which take two values: *1* for a conducting switch and *0* – for a non-conducting switch; *R*, *L* – resistance and inductance of inverter circuit, U_{dc} – input inverter voltage.

Upon transforming the system (9) of equations into the *d,q* frame:

$$\frac{d}{dt}\boldsymbol{I_{dq}} = \frac{1}{L}.\boldsymbol{U_{dq}} - \frac{R}{L}.\boldsymbol{I_{dq}} - \frac{U_R}{L}.\boldsymbol{P.S} - \boldsymbol{W.I_{dq}} =$$

$$= \frac{d}{dt}\boldsymbol{I_{inv}} = \boldsymbol{A_{inv}}.\boldsymbol{I_{inv}} + \boldsymbol{B_{inv}}.\boldsymbol{U} \qquad (10)$$

where: *P* – matrix of the *abc-dq0* frame transformation.

$$\boldsymbol{W} = \begin{bmatrix} 0 & -\omega_k \\ \omega_k & 0 \end{bmatrix} \qquad (11)$$

To connect the SynRM and inverter model, we need to calculate the voltage at the connection point. The voltage at the connection point of the motor and the inverter is calculated using Kirchhoff's first law in differential form, [6]:

$$\frac{d}{dt}\boldsymbol{I_{mot}} + \frac{d}{dt}\boldsymbol{I_{inv}} = \boldsymbol{A_{mot}}.\boldsymbol{I_{mot}} + \boldsymbol{B_{mot}}.\boldsymbol{U} + \boldsymbol{A_{inv}}.\boldsymbol{I_{inv}} + \boldsymbol{B_{inv}}.\boldsymbol{U} = \boldsymbol{0} \qquad (12)$$

We can use Kirchhoff's first law in differential form because these currents are continuous functions of time thanks to the fact that they are currents through inductances.

Substitution of the derivatives of the currents by the right-hand parts of the system of differential equations (8) turns the equations of the connections into an algebraic system of equations, which allows non-iterative calculation of the processes in the studied system. From where voltage at the connection point:

$$\boldsymbol{U} = -\frac{\boldsymbol{A_{mot}}.\boldsymbol{I_{mot}} + \boldsymbol{A_{inv}}.\boldsymbol{I_{inv}}}{\boldsymbol{B_{mot}} + \boldsymbol{B_{inv}}} \qquad (13)$$

4 Fault Simulation

The jammed rotor defect was implemented in Matlab environment. This is achieved by adding an unusually large load to it as it can be seen in Figure 4. The simulation starts with starting the bow thruster. It reaches its set reference speed of 1000RPM at around t=1s and when it is in steady state, the load disturbance is applied to the rotor shaft at t=2s. This simulation gives a direct reflection of the operational characteristics of the SynRM. The motor parameters are: L_d=0.05H, L_q=0.0051H, R_s=0.33Ohm, number of pole pairs - 2. Some of the obtained results are shown below.

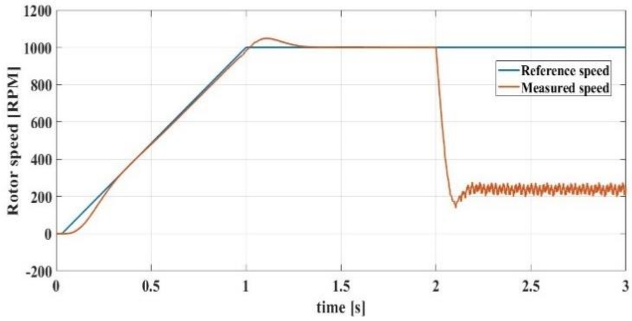

Fig. 4: SynRM rotor speed

The stator currents are shown in Figure 5. During the motor starting they reach around 250A and 700A when the disturbance is applied to the rotor.

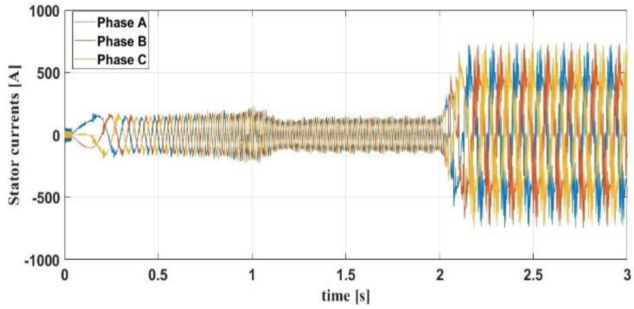

Fig. 5: SynRM stator currents

A time window with a period of 0.5s around the moment of rotor disturbance is shown on Figure 6.

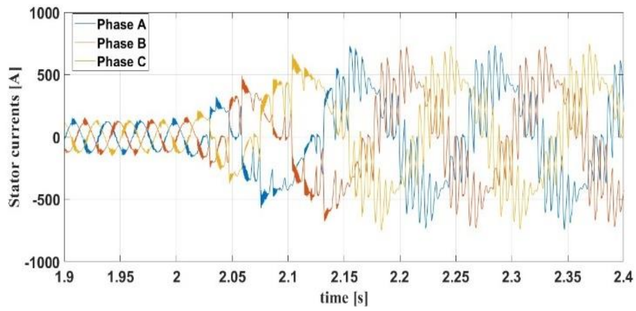

Fig. 6: Time window of SynRM stator currents

In Figure 7 can be seen the pulse width modulation waveform. A time window for the same period of time as for the stator currents waveform is shown in Figure 8.

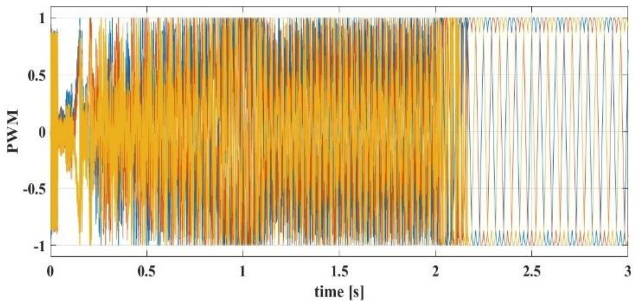

Fig. 7: PWM waveform

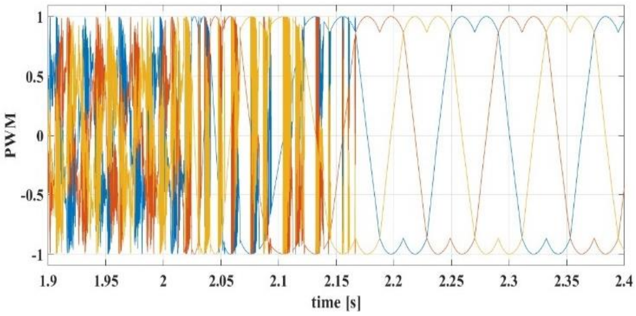

Fig. 8: Time window of PWM waveform

The currents of the motor in *d-q* frame are shown below. Figure 9 shows the current in *d*-axis and Figure 10 in *q*-axis respectively.

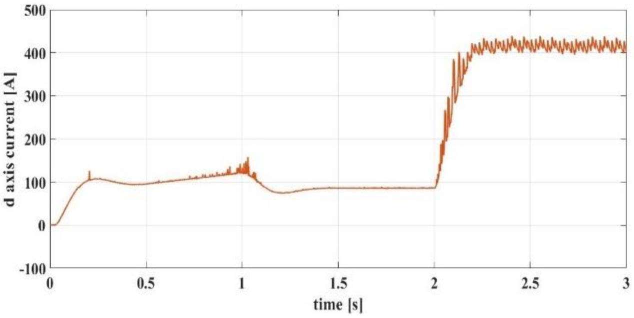

Fig. 9: D axis current

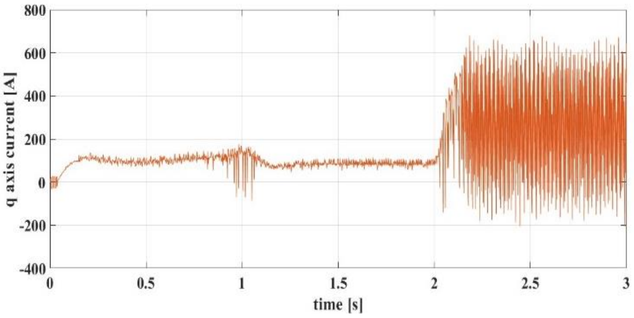

Fig. 10: Q axis current

Stator voltage curves in *d-q* frame are shown in Figure 11. With blue color is marked the voltage in *d* axis and with orange the voltage in *q* axis.

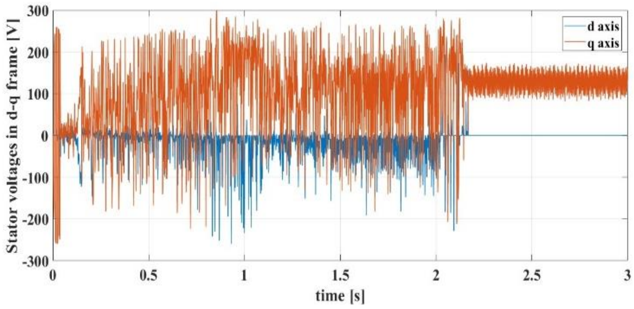

Fig. 11: Stator voltage in *d*,*q* frame

The measured and estimated torque of the bow thruster is shown in Figure 12. They are marked with blue and orange color respectively. It can be seen the large deviation after the moment when the disturbance is applied to the rotor.

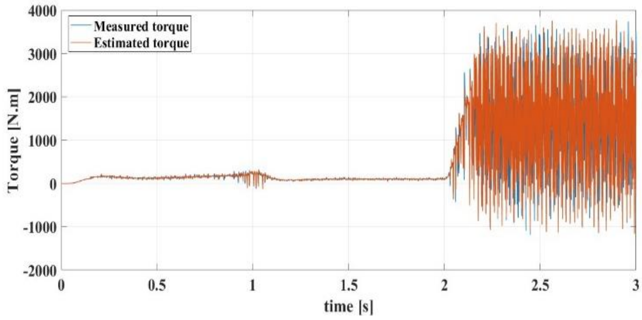

Fig. 12: SynRM torque

5 Machine Learning integration for Fault Diagnostics

We live in the time of the 5th Industrial Revolution. This is the time when artificial intelligence and technologies such as chatGPT will have an increasing influence on the modern world. Machine learning is a part of the science of artificial intelligence, which deals with the creation, examination, and research of mathematical models to discover similarities between different phenomena and events. Using implemented and validated mathematical models in the Matlab environment of electric drives, in particular SynRM, enough qualitative data can be collected about the state of the current, voltage, moment, etc. in defective conditions.

For this purpose, data from various simulations were collected and combined in one database. In this case, a csv file is used containing 4 different states - normal and three defectives. They are phase to housing, lack of phase, and jammed rotor. Each of these simulations is for a period of 3 seconds, with a frequency of 20,000hz, or in other words, 100,000 measurements of the three-phase currents for 1 simulation. Taken together they are a total of 220,000 measurements. They are labeled so that ML training can be aided, [34], [35], [36].

In Figure 13, one can see these points after some steps like clustering or de-numeration and extracting min-max bounds. In this case, a coefficient of 189 was used. To avoid overtraining and reducing the recognition success rate of the used classifiers.

The algorithm consisting of a total of 19 steps is implemented in the Python environment and uses the scikit-learn library for machine learning. In it, dozens of estimator models can be found that can be used. We have used only 21 of them here.

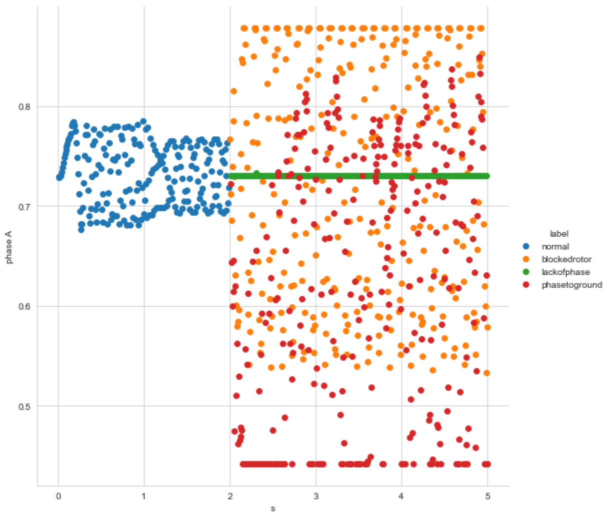

Fig. 13: Colored points of learning

Figure 14 shows a Nearest Centroid Classifier fusion matrix. It is a tool for evaluating the performance of estimators. For perfect results, there should be "hits" only on the diagonal of this 4x4 matrix. Here it is evident that there is a lot of scatter and therefore the success rate of this classifier for recognizing a defect such as a locked rotor is below 20%.

The report of the Random Forest classifier's work can be seen in Figure 15. This screenshot from Python shows again in text form a confusion matrix with a near-perfect result. There are several ways of assessment, such as precision, recall, and f1-score, depending on the approach adopted for calculation. The overall rating of this classifier is over 98% which is impressive.

The performance results of the 21 classifiers can be found in Figure 16. Such as Random Forest, Decision Tree, KNN and Bagging classifiers show excellent, close to perfect results. Other like Categorical NB and Bernoulli NB which are based on Bayes theorem show not-so-good results.

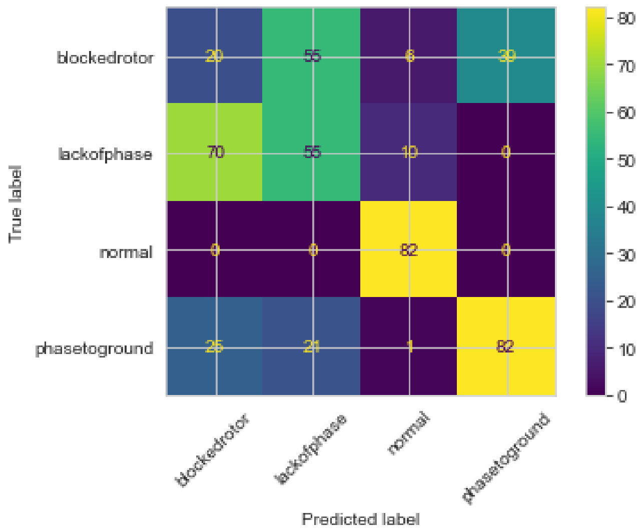

Fig. 14: Confusion matrix of Nearest Centoroid Classfier

```
[1165 rows x 5 columns]
Random Forest ->0
Confusion Matrix:
[[120   0   0   0]
 [  1 134   0   0]
 [  0   0  82   0]
 [  7   1   0 121]]
Classification Report: RandomForestClassifier()
               precision    recall  f1-score   support

 blockedrotor       0.94      1.00      0.97       120
  lackofphase       0.99      0.99      0.99       135
       normal       1.00      1.00      1.00        82
phasetoground       1.00      0.94      0.97       129

     accuracy                           0.98       466
    macro avg       0.98      0.98      0.98       466
 weighted avg       0.98      0.98      0.98       466

Accuracy: 0.98068669527897
```

Fig. 15: Text output from Python for Random Forest Classifier

There are different methods for calculating the training accuracy of machine learning classifiers, such as precision, recall, and f1-score. They interpret the data differently by taking into account the total, correct, and incorrect recognition attempts, [37], [38]

$$\text{For Example } \boldsymbol{Precision} = \frac{\boldsymbol{TP}}{\boldsymbol{TP+FP}} \quad (14)$$

where TP is the number of cases correctly predicted as positive by the classifier model and FP is the number of cases which were incorrectly predicted as positive by the classifier model.

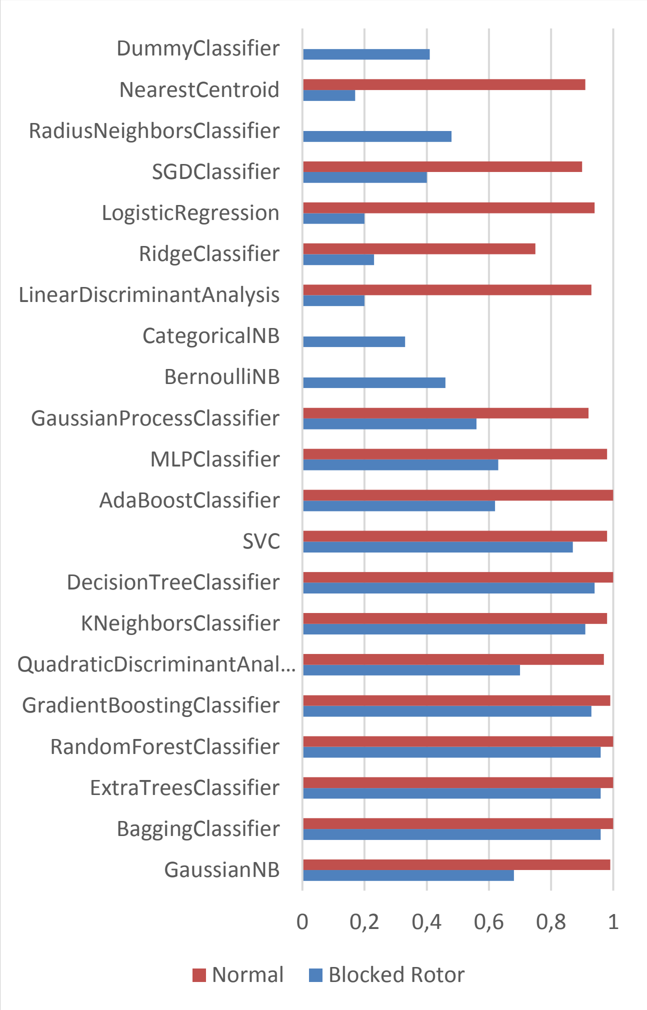

Fig. 16: Success rate of different classifiers

6 Conclusion

In this report, a common problem with electric drives and in particular the jamming of the rotor of synchronous reluctance motor was presented. For this purpose, a flexible mathematical model of this type of electric motor was compiled, in which defects of different types and characteristics can be easily simulated.

During these simulations, data was collected on various operating parameters such as stator current, torque, rotational speed, etc. as the simulation is for a period of 3 seconds and a data frequency of 20khz.

The data collected during these simulations were used for diagnostics by using artificial intelligence and in particular the method of machine learning. For this purpose, an algorithm consisting of 18 basic steps has been implemented, which uses the current values at different times for its training. More than 20 different types of classifiers and regressions are used in this algorithm. As a result, clear information is obtained about the possibilities of using ML for the diagnosis of SynRM. As can be seen from the demonstrated results, some classifiers achieve a success rate of over 98%, which is remarkable, considering that no optimization has yet been performed, after which the success rate would increase to over 99.5%.

Optimizations that could be performed and are currently the subject of our current research are optimization of the number of input data, optimization of training boundaries, and optimization of the parameters of ML classifiers. The results of these will be published in subsequent publications. The main goal of these optimizations is to achieve maximum accuracy with optimal training time.

Acknowledgement:
The study was funded by the Bulgarian Research Fund, Competition for Financial Support for Basic Research Projects 2021, Project title: “Integrated wireless sensor networks for diagnostics of ship electrical equipment”

References:
[1] R.-R. *Moghaddam, Synchronous Reluctance Machine (SynRM) in Variable Speed Drives (VSD) Applications. Theoretical and Experimental Reevaluation,* PhD Thesis, Royal Institute of Technology (KTH), Stockholm, Sweden 2011, p.260.
[2] H. Heidari, A. Rassolkin, A. Kallaste, T. Vaimann, E. Andriushchenko, A. Belahcen, D.V. Lukichev, *A review of synchronous reluctance motor-drive advancements, MDPI Sustainability*, 2021, Vol.13, 729, p.37. doi: 10.3390/su13020729.
[3] Isermann R., *Detection to Fault Tolerance,* 2006, Springer, p.475. ISBN: 9783540303688.
[4] R. Isermann, Fault-Diagnosis Applications. Model-Based Condition Monitoring: Actuators, Drives, Machinery, Plants, Sensors, and Fault-tolerant Systems, 2011, Springer, p.372. ISBN: 978-3-642-12766-3.
[5] W.T. Thomson, I. Culbert, Current Signature Analysis for Condition Monitoring of Cage Induction Motors. Industrial Application and Case Histories, 2000, John Wiley & Sons, p.426. ISBN: 978-1-119-02959-5.
[6] Electrical Machines Diagnosis, Edited by Jean-Claude Trigeassou, 2011, John Wiley & Sons, p.344. ISBN: 978-1-84821-263-3.

[7] H. Toliyat, S. Nandi, S. Choi, H. Meshgin-Kelk, Electric machines. Modeling, Condition Monitoring and Fault Diagnosis, 2013, Taylor & Francis, p.266. ISBN: 978-1-4200-0628-5.

[8] Induction Motors. Applications, Control and Fault Diagnostics, Edited by Raul Igmar Gregor Recalde, 2015, AvE4EvA, p.383. ISBN-10: 953-51-2207-X

[9] J. Faiz, V. Ghorbanian, G. Joksimović, Fault Diagnosis of Induction Motors, 535 p. The Institution of Engineering and Technology, 2017, ISBN: 978-1-78561-329-6.

[10] Diagnosis and Fault Tolerance of Electrical Machines, Power Electronics and Drives, Edited by Antonio J. Marques Cardoso, 2018, The Institution of Engineering and Technology, p.373. ISBN: 978-1-78561-532-0.

[11] P. Tavner, L. Ran. C. Crabtree, Condition Monitoring of Rotating Electrical Machines, 3rd Edition, 2020, The Institution of Engineering and Technology, p.434. ISBN: 978-1-78561-866-6

[12] N. Saad, M. Irfan, R. Ibrahim, Condition Monitoring and Faults Diagnosis of Induction Motors. Electrical Signature Analysis, 2019, Taylor & Francis, p.171. ISBN: 9781351172561.

[13] J. Chen, R.J. Patton, Robust Model-Based Fault Diagnostis for Dynamic Systems, 1999, Kluwer, p.350. ISBN: 0-7923-8253-6.

[14] R.J. Patton, P.M. Frank, R.N. Clark, lssues of Fault Diagnosis for Dynamic Systems, 2000, Springer, p.612. ISBN: 978-1-84996-995-6.

[15] S. Simani, C. Fantuzzi, R.J. Patton, Modeling-Based Fault Diagnosis in Dynamic Systems using Identification Techniques, 2002, Springer, p.291. ISBN: 978-1-4471-3829-7.

[16] J. Korbicz· J.M. Koscielny, Z. Kowalczuk, W. Cholewa, Fault Diagnosis Models, Artificial Intelligence, Applications, 2004, Springer, p.935. ISBN: 978-3-642-62199-4.

[17] C.M. Bishop, Pattern Recognition and Machine Learning, 2006 Springer, p.758. ISBN-10: 0-387-31073-8.

[18] G. Vachtsevanos, F. Lewis, M. Roemer, A. Hess, B. Wu, Intelligent fault diagnosis and prognosis for engineering systems, 2006, John Wiley & Sons, p.434. ISBN-10: 0-471-72999-X.

[19] Unsupervised Process Monitoring and Fault Diagnosis with Machine Learning Methods A.C. Müller, S. Guido, Introduction to Machine Learning with Python. A Guide for Data Scientists, 2017, O'Reilly, p.392. ISBN: 978-1-449-36941-5.

[20] N. Bianchi, C. Babetto, G. Bacco, Synchronous Reluctance Machines. Analysis, optimization and applications, 2021, The Institution of Engineering and Technology, p.352. ISBN: 978-1-83953-264-1.

[21] H. Heidari, A. Rassõlkin, A. Kallaste, T. Vaimann, E. Andriushchenko, A. Belahcen , D.V. Lukichev, A review of synchronous reluctance motor-drive advancements, MDPI Sustainability, 2021, Vol.13, 729, p.37. doi: 10.3390/su13020729.

[22] I.Ch. Proimadis, D.V. Spyropoulos, E.D. Mitronikas, "An alternative for all-electric ships applications: The synchronous reluctance motor," Hindawi Journal Advances in Power Electronics, Vol.2, No.13, Article ID 862734, p.7. doi: 10.1155/2013/862734.

[23] G. Boztas, O. Aydogmus, "Implementation of sensorless speed control of synchronous reluctance motor using extended Kalman filter," *Engineering Science and Technology, an International Journal*, Vol.31, July 2022, 101066, 7 p. doi: 10.1016/j.jestch.2021.09.012.

[24] P. Neti, S. Nandi, "Performance analysis of a reluctance synchronous motor under abnormal operating conditions," *Canadian Journal of Electrical and Computer Engineering,* Vol.33, No.2, Spring 2008, pp.55-61. doi: 10.1109/CJECE.2008.4621830.

[25] P.C. Krause, O. Wasynczuk, S.D. Sudhoff, S. Pekarek Analysis of Electric Machinery and Drive Systems, 3rd Edition, 2013, John Wiley & Sons, p.676 p. ISBN: 047114326X.

[26] G. Enchev, "Fault Diagnostics of Induction Motors on Bord Vessel Using AI Optimized Computer," *2023 15th Electrical Engineering Faculty Conference (BulEF),* Varna, Bulgaria, 2023, pp. 1-5, doi: 10.1109/BulEF59783.2023.10406249.

[27] H. Milushev, G. Enchev and N. Djagarov, "Simulating a Lack of Phase Fault on SynRM and Integrate Results with Machine Learning," *2023 International Conference Automatics and Informatics (ICAI),* Varna, Bulgaria, 2023, pp. 18-22, doi: 10.1109/ICAI58806.2023.10339049.

[28] G. Enchev, "Detailed Investigation of ML Algoritms for Diagnostics of IM on Board

Vessel," *2023 International Conference Automatics and Informatics (ICAI),* Varna, Bulgaria, 2023, pp. 32-36, doi: 10.1109/ICAI58806.2023.10339028.

[29] R.E. Betz, „Theoretical aspects of control of synchronous reluctance machines," IEE Proceedings B: Electric Power Applications, Vol.139, No. 4. July 1992, pp.355-364. doi: 10.1049/ip-b.1992.0042.

[30] V. Aguba, M. Muteba, D.V. Nicolae, "Dynamic modelling and transient analysis of synchronous reluctance motor with cage bars in the rotor structure," *IEEE International Symposium on Power Electronics, Electrical Drives, Automation and Motion (SPEEDAM),* 20-22 June 2018, Amalfi, Italy. doi: 10.1109/SPEEDAM.2018.8445292.

[31] S. Yamamoto, T. Kojima, H. Hirahara, "Mathematical models of synchronous reluctance motor considering iron loss and cross-magnetic saturation with reciprocity relation of mutual inductance," *IEEJ Journal of Industry Applications,* Vol.11 No.1, 2022, pp.206–215. doi: 10.1541/ieejjia.21001783

[32] N.F. Djagarov, "A method of transient electromechanical processes modeling in power systems," *Proceedings of 2009 IEEE Bucharest PowerTech Conference,* June 28th - July 2nd, Bucharest, Romania, art. No.5281949, p.6. doi: 10.1109/PTC.2009.5281949

[33] Q.-T. An, L.-Zh. Sun, K. Zhao, L.i Sun, Switching function model-based fast-diagnostic method of open-switch faults in inverters without sensors, *IEEE Transactions on Power Electronics,* Vol.26, No.1, January 2011, pp.119-126. doi: 10.1109/TPEL.2010.2052472

[34] G. Panayotova, G. P. Dimitrov, P. Petrov and B. Os, "Modeling and data processing of information systems," *2016 Third International Conference on Artificial Intelligence and Pattern Recognition (AIPR),* Lodz, Poland, 2016, pp. 1-5, doi: 10.1109/ICAIPR.2016.7585229.

[35] V. Martsenyuk, G. Dimitrov, D. Rancic, I. Dirgova-Luptakova. I. Jovancevic, A. Klos-Wiktowska, M. Bernas, T. Gancarczyk, "On Emerging Methodology for Collection of Good Practices in the Area of Applied Artificial Intelligence," *2023 16th International Conference on Advanced Technologies, Systems and Services in Telecommunications (TELSIKS),* Nis, Serbia, 2023, pp. 277-283, doi: 10.1109/TELSIKS57806.2023.10316104.

[36] I. Ahmed, G. Jeon and F. Piccialli, "From Artificial Intelligence to Explainable Artificial Intelligence in Industry 4.0: A Survey on What, How, and Where," in *IEEE Transactions on Industrial Informatics,* vol. 18, no. 8, pp. 5031-5042, Aug. 2022, doi: 10.1109/TII.2022.3146552.

[37] Precision, Recall, and F1 Score: A Practical Guide Using Scikit-Learn. Proclus Academy, [Online]. https://proclusacademy.com/blog/practical/precision-recall-f1-score-sklearn/ (Accessed Date: December 10, 2024).

[38] F1 Score in Machine Learning. Geeks for Geeks, [Online]. https://www.geeksforgeeks.org/f1-score-in-machine-learning/ (Accessed Date: December 10, 2024).

Contribution of Individual Authors to the Creation of a Scientific Article (Ghostwriting Policy)

The authors equally contributed in the present research, at all stages from the formulation of the problem to the final findings and solution.

Sources of Funding for Research Presented in a Scientific Article or Scientific Article Itself

The study was funded by the Bulgarian Research Fund, Competition for Financial Support for Basic Research Projects 2021, Project title: "Integrated wireless sensor networks for diagnostics of ship electrical equipment".

Conflict of Interest

The authors have no conflicts of interest to declare.